Carcinogenesis, 2019, 1–10

doi:10.1093/carcin/bgz135
Advance Access publication 29 July, 2019
Original Article

ORIGINAL ARTICLE

Unique miRNA profiling of squamous cell carcinoma arising from ovarian mature teratoma: comprehensive miRNA sequence analysis of its molecular background

Kosuke Yoshida[1,2], Akira Yokoi[1,3], Takumi Kagawa[2], Shingo Oda[2], Satomi Hattori[1], Satoshi Tamauchi[1], Yoshiki Ikeda[1], Nobuhisa Yoshikawa[1], Kimihiro Nishino[1], Fumi Utsumi[4], Kaoru Niimi[1], Shiro Suzuki[1], Kiyosumi Shibata[4], Hiroaki Kajiyama[1,*], Tsuyoshi Yokoi[2] and Fumitaka Kikkawa[1]

[1]Department of Obstetrics and Gynecology and [2]Department of Drug Safety Sciences, Division of Clinical Pharmacology, Nagoya University Graduate School of Medicine, Nagoya, Japan, [3]Department of Gynecologic Oncology and Reproductive Medicine, The University of Texas MD Anderson Cancer Center, Houston, TX, USA and [4]Department of Obstetrics and Gynecology, Fujita Health University Bantane Hospital, Nagoya, Japan

*To whom correspondence should be addressed. Tel: +81 52 744 2261; Fax: +81-52-744-2268; Email: kajiyama@med.nagoya-u.ac.jp

Abstract

Owing to its rarity, the carcinogenesis and molecular biological characteristics of squamous cell carcinoma arising from mature teratoma remain unclear. This study aims to elucidate the molecular background of malignant transformation from the aspects of microRNA (miRNA) profiling. We examined 7 patients with squamous cell carcinoma and 20 patients with mature teratoma and extracted their total RNA from formalin-fixed paraffin-embedded tissues. Then we prepared small RNA libraries and performed comprehensive miRNA sequencing. Heatmap and principal component analysis revealed markedly different miRNA profiling in cancer, normal ovarian and mature teratoma tissues. Then we narrowed down cancer-related miRNAs, comparing paired-cancer and normal ovaries. Comparisons of cancer and mature teratoma identified two markedly upregulated miRNAs (miR-151a-3p and miR-378a-3p) and two markedly downregulated miRNAs (miR-26a-5p and miR-99a-5p). In addition, these findings were validated in fresh cancer tissues of patient-derived xenograft (PDX) models. Moreover, several miRNAs, including miR-151a-3p and miR-378a-3p, were elevated in the murine plasma when tumor tissues were enlarged although miR-26a-5p and miR-99a-5p were not elucidated in the murine plasma. Finally, we performed target prediction and functional annotation analysis *in silico* and indicated that targets genes of these miRNAs markedly correlated with cancer-related pathways, including 'pathway in cancer' and 'cell cycle'. In conclusion, this is the first study on miRNA sequencing for squamous cell carcinoma arising from mature teratoma. The study identified four cancer-related miRNAs that were considered to be related to the feature of malignant transformation. Moreover, miRNAs circulating in the murine plasma of the PDX model could be novel diagnostic biomarkers.

Introduction

Mature teratoma (MT) of the ovary is one of the leading ovarian tumors, comprising nearly 20% of all ovarian neoplasms (1–3). However, the malignant transformation of MT is sporadic, occurring in nearly 1–3% of all MT cases (2,3). Squamous cell carcinoma (SCC) is the leading form of malignant transformation (75–90%), although any histological subtypes could occur (2–4). Despite its histology, the malignant transformation of MT is classified in germ cell tumors and considered to be different from epithelial ovarian cancers (5). Typically, SCC arising from MT (SCC-MT) is reported in postmenopausal women; thus,

Received: February 19, 2019; **Revised:** June 23, 2019; **Accepted:** July 27, 2019

Abbreviations

FFPE	formalin-fixed paraffin-embedded
miRNA	microRNAs
MT	mature teratoma
PDX	patient-derived xenograft
qPCR	quantitative polymerase chain reaction
SCC	squamous cell carcinoma.

several preoperative predictors, such as age (>45 years), tumor size (>99 mm) and the level of SCC antigen (>1.5 ng/ml) have been proposed (2,6). However, distinguishing early-stage SCC-MT from MT preoperatively remains challenging, and some patients have been incidentally diagnosed postoperatively. Reportedly, the standard treatment comprises the maximum debulking surgery; however, consensus is lacking regarding adjuvant treatment (2,7–10). Thus, the prognosis of patients who could not undergo complete surgery remains poor, and mean survival period of patients who did not have a hysterectomy is 15.8 months (2). Hence, early diagnosis is imperative, and novel preoperative potential biomarkers are desired. Nevertheless, limited preliminary studies have been conducted because of the low incidence of SCC-MT (11–15), and carcinogenesis and molecular biological characteristics of this malignancy remain mostly unclear.

MicroRNAs (miRNAs), small non-coding RNA molecules (~22 nucleotides in length), regulate the gene expression post-transcriptionally and play multiple roles in physiology, exhibiting functions such as tumor-suppressor genes or oncogenes (16–21). Recently, next-generation sequencing (NGS) has been widely acknowledged as a novel technology that facilitates obtaining a comprehensive miRNA landscape (22). In addition, extracellular RNA has garnered considerable attention as a non-invasive biomarker, and previous studies have suggested that several extracellular miRNAs could be potential diagnostic biomarkers of early-stage epithelial ovarian cancer (23,24). Hence, investigating miRNAs could elucidate the disease pathogenesis and facilitate the identification of novel non-invasive biomarkers.

To the best of our knowledge, this is the first study to investigate the miRNA profiling in SCC-MT using NGS.

Materials and methods

Patients

We retrospectively reviewed the medical records of patients with ovarian carcinoma who were treated at Nagoya University Hospital (Aichi, Japan) between 2003 and 2016. We identified all the seven patients with SCC-MT who underwent surgery without neoadjuvant therapy (cases 1–7); formalin-fixed paraffin-embedded (FFPE) cancer and contralateral normal ovarian tissues of these patients were used in this study. In addition, we randomly selected 20 patients with MT who underwent surgery in the same period (cases 8–27) and used their FFPE tumors as a control. In addition, as the control for the patient-derived xenograft (PDX) model, we used most recent fresh-frozen surgical specimens (cases 28 and 29, MT tissues; case 30, normal ovarian tissues of patients with mucinous cystadenoma; case 31, normal ovarian tissues of patients with stroma). This study protocol was approved by the ethics committee of our institute (approval nos. 2015-0237, 2017-0053 and 2017-0497). We obtained written informed consent from all patients.

PDX model mice

We established PDX mouse models from two patients (cases 5 and 7), and there were only two patients with SCC-MT after the start of research using PDX model. Briefly, we obtained fresh surgical tissue, sectioned into ~3 mm^3 pieces and implanted subcutaneously into a 5-week-old female NOD.Cg-*Prkdc*^{scid}*Il2rg*^{tm1Wjl}/SzJ (NSG) (Charles River Laboratories Japan, Kanagawa, Japan). The generation harboring the patient-derived material was termed F_1, with subsequent generations numbered consecutively (F_2, F_3, F_4 and so on). In this study, we used fresh-frozen cancer tissues of case 5-F_2, case 7-F_3, and an original fresh-frozen surgical sample of case 7.

We used 5-week-old female Balb/c-nu/nu mice (Charles River Laboratories), to investigate the plasma miRNA. Under isoflurane anesthesia, we reimplanted cancer tissues of case 5-F_2 into five mice subcutaneously and collected blood from the eye fundus sequentially (1 week before, 1 and 3 weeks after implantation) using a 2K-EDTA capillary tube (Vitrex Medical A/S, Herlev, Denmark). At 5 weeks post-implantation, we killed mice and collected blood via cardiac puncture. Then the blood was centrifuged, pooled and used for further analyses.

RNA extraction and miRNA sequencing

In this study, we used archival FFPE cancer, contralateral normal ovarian tissues of SCC-MT patients and MT tissues of other patients. FFPE blocks of cancer contained at least > 60% of cancer tissues pathologically. The total RNA was extracted from eight 5-μm thick sections of the blocks using the miRNeasy FFPE Kit (Qiagen, Hilden, Germany). In addition, we used fresh SCC-MT tissues, plasma of the PDX model and fresh MT tissues of other patients and extracted the total RNA using the miRNeasy Mini Kit or the miRNeasy Serum/Plasma Kit (Qiagen). The total RNA concentration of each sample was measured using NanoDrop (Thermo Fisher Scientific, Waltham, MA). We prepared small RNA libraries using the NEBNext Multiplex Small RNA Library Prep Set for Illumina (New England Biolabs, Ipswich, MA) and added index codes to attribute sequences to each sample. Next, PCR products were purified using the QIAquick PCR Purification Kit (Qiagen) and 6% TBE gel (120 V, 60 min). Furthermore, DNA fragments corresponding to 140–160 bp (the length of small non-coding RNA plus the 3′ and 5′ adaptors) were recovered, and the complementary DNAs concentration was measured using the Qubit dsDNA HS Assay Kit and a Qubit2.0 Fluorometer (Life Technologies, Carlsbad, CA). Finally, single-end reads were performed on the Illumina MiSeq (Illumina, San Diego, CA).

Data analysis

The CLC Genomics Workbench version 9.5.3 program (Qiagen) was used for data analysis. First, adaptor sequences were trimmed, and sequences between 15 and 35 bps were counted. Then, the trimmed data were mapped to the miRbase 21 database, allowing up to two mismatches (25). After the normalization using reads per million mapped reads, low-expression (<10 reads in all samples) miRNAs were excluded from all samples. Then RStudio (RStudio, Boston, MA) and R software (ver. 3.5.0) were used for further analysis. We converted the normalized data to base 10 logarithms and *z*-scores and performed clustering and principal component analysis. For the clustering analysis, the distance was calculated as '1 – Spearman correlation coefficient', and the 'ward.D2' clustering method was used. To generate a heatmap, we used the heatmap.2 function of the gplots package (ver. 3.0.1) given in the R software and omitted miRNAs whose normalized value was <1000 reads in all samples. To calculate and visualize principal component analysis, we used the prcomp and the plot3d functions of the rgl package (ver. 0.99.16) given in the R software. For the murine plasma, both mmu-miRNAs and hsa-miRNAs were annotated, and heatmap analysis was performed for hsa-miRNAs, excluding mmu-miRNAs.

Comparing the normalized expression values of paired-cancer and normal tissues, we investigated SCC-MT–related dysregulated miRNAs. We used the difference of >1000 reads as the cut-off, and the dysregulated miRNAs in six or more cases were extracted using Venn diagrams. Then, comparing seven SCC-MT tissues and 20 MT tissues by a *t*-test using RStudio, we identified miRNAs that were markedly more dysregulated in SCC-MT than in MT tissues. Likewise, miRNAs, which were markedly more dysregulated in MT than in normal tissues, were identified.

Enzyme-linked immunosorbent assay

We measured the murine plasma SCC antigen using the SCCA-LISA ELISA Kit (Xeptagen SpA, Italy). In addition, pooled plasma samples of each point were diluted three times by a dilution buffer of the kit. All samples were performed in duplicate.

Quantitative polymerase chain reaction

We performed quantitative polymerase chain reaction (qPCR) using mice plasma of PDX model. Briefly, complementary DNAs was synthesized using TaqMan™ Advanced miRNA cDNA Synthesis Kit (Thermo Fisher Scientific) according to the manufacturer's instructions. TaqMan® Fast Advanced Master Mix (Thermo Fisher Scientific) and TaqMan™ Advanced miRNA Assay (Assay ID 477919_mir for hsa-miR-151a-3p and Assay ID 478349_mir for hsa-miR-378a-3p; Thermo Fisher Scientific) were used. Then, qPCR was performed using an M×3000P (Agilent Technologies, Santa Clara, CA), and the PCR conditions included denaturation at 95°C for 10 min, followed by 40 amplification cycles of 95°C for 15 s and 60°C for 1 min. The amplified product was monitored by measuring the increase of the FAM fluorescence intensity.

In silico analysis

We used the miRSystem (http://mirsystem.cgm.ntu.edu.tw/) to perform target prediction and functional annotation in one step (26). First, target genes that were found in ≥3 of seven databases in the miRSystem (miRanda, PicTar, DIANA, miRBridge, rna22, PITA and TargetScan) were identified. Then, we conducted the Kyoto Encyclopedia of Genes and Genomes pathway enrichment analysis for target genes with an expected ratio of ≥2. In addition, we used TarBase v8–DIANA tools (http://carolina.imis.athena-innovation.gr/diana_tools/web/index.php?r=tarbasev8%2Findex) which provides data about experimentally validated miRNA–gene interactions.

Results

Identification of SCC-MT–related miRNA

We used FFPE tissues of patients with SCC-MT or MT. Table 1 summarizes the characteristics of patients with SCC-MT. The median age was 55 (range, 31–64) years, and the median serum SCC antigen level was 3.5 (range, 2.5–17.9) ng/ml. All patients underwent surgery, followed by combination chemotherapy. Only one patient (case 5) experienced recurrence and died of the disease. Figure 1 shows representative images of hematoxylin and eosin stains of SCC-MT. The cancer tissue of case 2 was apparently keratinizing-type SCC, and the area of cancer cells was relatively small. In addition, the cancer tissue of cases 6 and 7 contained necrotic tissues, whereas the cancer tissue from two PDX mice models displayed characteristics of SCC well. Conversely, the median age of 20 patients with MT was 38 (range, 21–72) years, and their median serum SCC antigen level was 1.3 (range, 0.5–2.4) ng/ml.

We extracted the total RNA from archived FFPE tissues of cancer and contralateral normal ovaries of patients with SCC-MT. In addition, FFPE tissues of MT tissues of other patients were used as a control. Then miRNA sequencing was performed, and the mean annotated row read counts were 535 365 reads. The heatmap analysis revealed miRNA expression profiles differing from each other (Figure 2A). Although normal ovarian tissues exhibited almost similar profiles, SCC-MT tissues differed from each other. In addition, five MT tissues (MT-23 to MT-27) were similar to that of normal tissues, and 13 MT tissues (MT-10 to MT-22) displayed almost similar profiles. However, two MT tissues (MT-8 and MT-9) were classified in a cluster that included SCC-MT tissues. We observed a similar tendency in the principal component analysis (Figure 2B). In this study, miRNAs were classified into three main groups as follows: group-A comprised miRNAs more highly expressed in SCC-MT than in the other tissues; group-B comprised miRNAs more highly expressed in SCC-MT and MT than in normal tissues; group-C comprised miRNAs more poorly expressed in SCC-MT than in other tissues (Figure 2A).

We compared the normalized expression reads of paired-cancer and normal tissues to narrow down SCC-MT–related miRNAs. Three and nine miRNAs were commonly upregulated in stage I and stage II patients, respectively. Of those, seven miRNAs, which were upregulated in six or more cases, were defined as upregulated miRNAs in SCC-MT (miR-22-3p, miR-146a-5p, miR-151a-3p, miR-200b-3p, miR-205-5p, miR-221-3p and miR-378a-3p) in SCC-MT (Figure 3A). Likewise, 11 and 6 miRNAs, which were frequently downregulated in stage I and stage II patients, respectively, and 8 miRNAs, which were downregulated in six or more cases, were defined as downregulated miRNAs in SCC-MT (miR-10b-5p, miR-26a-5p, miR-99a-5p, miR-100-5p, miR-125a-5p, miR-125b-5p, miR-143-3p and miR-145-5p; Figure 3B). Then we compared the normalized expression values of 15 dysregulated miRNAs in 7 SCC-MT and 20 MT tissues statistically. Consequently, miR-151a-3p and miR-378a-3p were significantly upregulated ($P = 0.046$ and $P = 0.016$, respectively), and miR-26a-5p and miR-99a-5p were significantly downregulated ($P \leq 0.001$ and $P = 0.008$, respectively) in SCC-MT compared with those in MT tissues (Figure 3C). Likewise, 20 MT and 7 normal tissues were also compared statistically; 8 miRNAs, which were significantly dysregulated in MT than normal tissues, were identified (miR-200b-3p***, miR-205-5p***, miR-378a-3p***, miR-221-3p**, miR-146a-5p*, miR-10b-5p**, miR-145-5p** and miR-143-3p*; *$P \leq 0.05$, **$P \leq 0.01$ and ***$P \leq 0.001$; Figure 3C).

Validation of SCC-MT–related miRNA using the PDX model

To validate the results of the FFPE tissues, we used fresh-frozen SCC-MT tissues of case 7 and the two PDX mice models. Moreover, fresh surgical specimens of MT and normal ovaries of other patients as a control. MiRNA sequencing revealed that

Table 1. Patients' characteristics

Case	Age	FIGO	Histology	Serum SCC antigen level(ng/ml)	Initial treatment		Outcome
					Surgery	Chemotherapy	
1	38	IA	SCC	2.8	Left cystectomy → LSO	TC	NED
2	55	IC1	SCC	11.5	ATH + BSO + OM + PEN (sampling)	PF	NED
3	62	IC1	SCC	3.5	ATH + BSO + OM	TC	NED
4	64	IC2	SCC	9.8	ATH + BSO + OM + PEN	TC	NED
5	31	IIA	SCC	17.9	RSO + left cystectomy + OM → ATH + LSO	PF	DOD
6	37	IIB	SCC	6.4	ATH + BSO + OM	PF	NED
7	64	IIB	SCC	2.5	ATH + BSO + rectal and right ureter resection	PF	NED

ATH, abdominal total hysterectomy; BSO, bilateral salpingo-oophorectomy; DOD, died of disease; FIGO, International Federation of Gynecology and Obstetrics; LSO, left salpingo-oophorectomy; NED, no evidence of disease; OM, omentectomy; PEN, pelvic lymph-node dissection; PF, cisplatin and 5-FU; RSO, right salpingo-oophorectomy; SCC, squamous cell carcinoma; TC, paclitaxel and carboplatin.

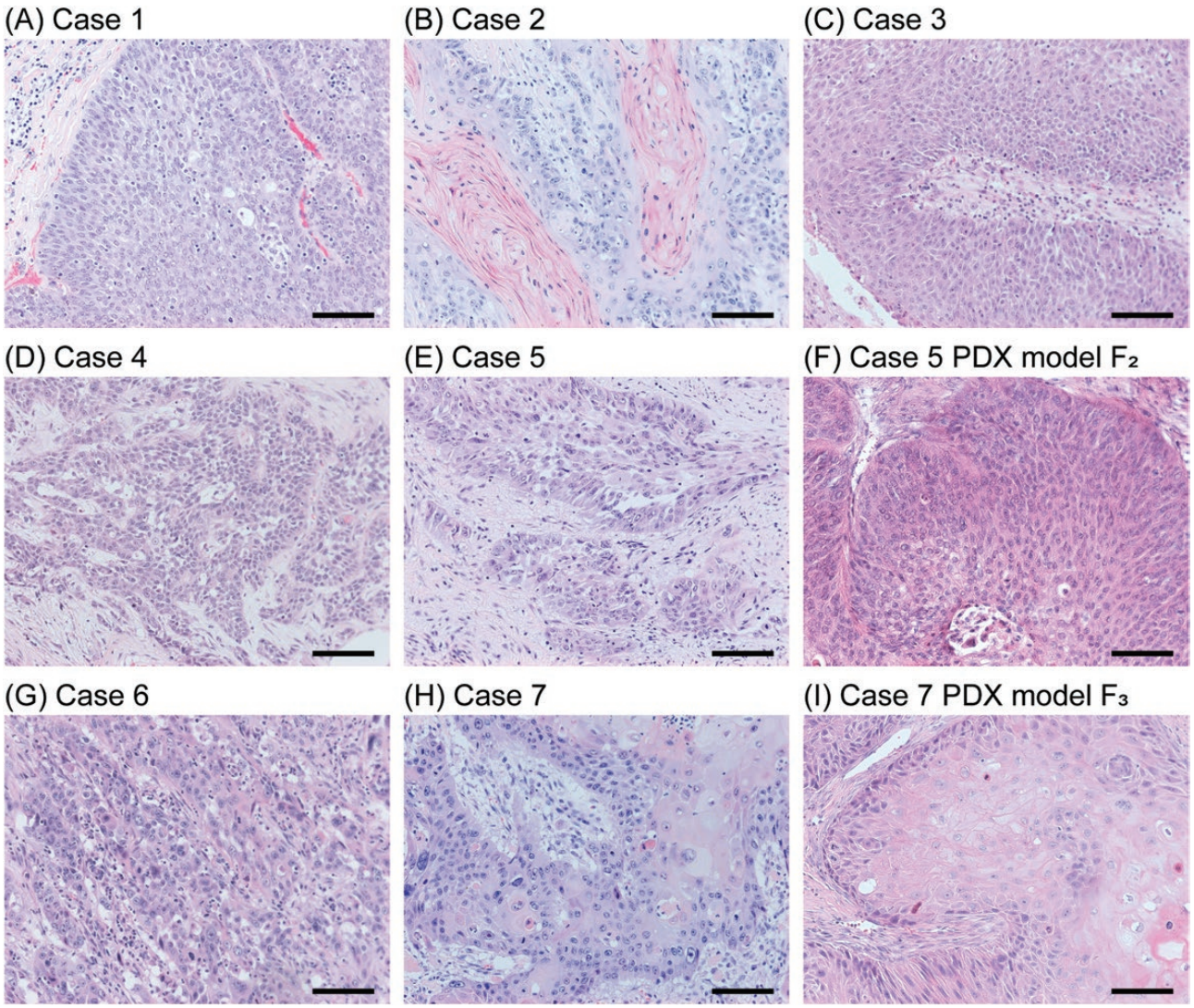

Figure 1. Representative images of cancer tissues. Hematoxylin and eosin staining of cancer tissues of patients (**A–E**, **G** and **H**), and PDX model (**F** and **I**). Scale bars, 100 μm.

miRNAs profiling in the fresh-frozen cancer tissues correlated well with the original FFPE tissues (Figure 3D). The heatmap analysis revealed that three fresh-frozen SCC-MT tissues (case 7, PDX case 5-F_2 and case 7-F_3) exhibited almost similar expression profiles (Figure 4A). In addition, expression profiles of one MT tissue (MT-29) corroborated those of normal tissues, whereas the other MT tissue (MT-28) varied from those of normal tissues. In addition, the 7 upregulated and 8 downregulated miRNAs identified in Figure 3A and B are shown on the right side of Figure 4A. Consequently, most dysregulated miRNAs were also dysregulated in fresh SCC-MT tissues of the PDX model. Nevertheless, hsa-miR-151a-3p was not upregulated in case 7 and PDX model case 7-F_3. Furthermore, all downregulated miRNAs were downregulated in fresh SCC-MT compared with MT and normal tissues. Hence, the result of fresh-frozen tissues correlated with that of FFPE tissues (Figures 2A and 4A).

In this study, we investigated the plasma miRNA of the PDX model to determine whether these miRNAs could be specific biomarkers for SCC-MT. The cancer tissues of case 5-F_2 were reimplanted subcutaneously into five nude mice, and the plasma was obtained sequentially. We observed no apparent tumors at 1 week post-implantation. Then tumors were palpable at 3 weeks post-implantation and increased rapidly. MiRNA sequencing revealed that several miRNAs, including hsa-miR-378a-3p and miR-151a-3p, elevated at 5 weeks post-implantation (Figure 4B). Moreover, several miRNAs were downregulated in the meanwhile, although hsa-miR-26a-5p and miR-99a-5p were not annotated at any point of the murine plasma. Hence, we focused on upregulated miRNAs in the murine plasma and assessed sequential normalized reads of the top 8 miRNAs that had >100 reads at 5 weeks post-implantation. Analogous to the heatmap in Figure 4B, most miRNAs rapidly elevated between 3 and 5 weeks post-implantation (Figure 4C). In addition, the plasma SCC antigen rapidly elevated (9.3 ng/ml) at 5 weeks post-implantation. Conversely, some miRNAs, such as hsa-miR-320b, miR-139-5p and miR-378a-3p, marginally elevated at 1 and 3 weeks post-implantation when the plasma SCC antigen level was still below the reference value (2.0 ng/ml). Furthermore, hsa-miR-1246 and miR-1290 levels were remarkably elevated, compared with the elevation of the plasma SCC antigen level and other miRNAs. Regarding miR-151a-3p and miR-378a-3p, the results of miRNA sequencing were validated by qPCR, and

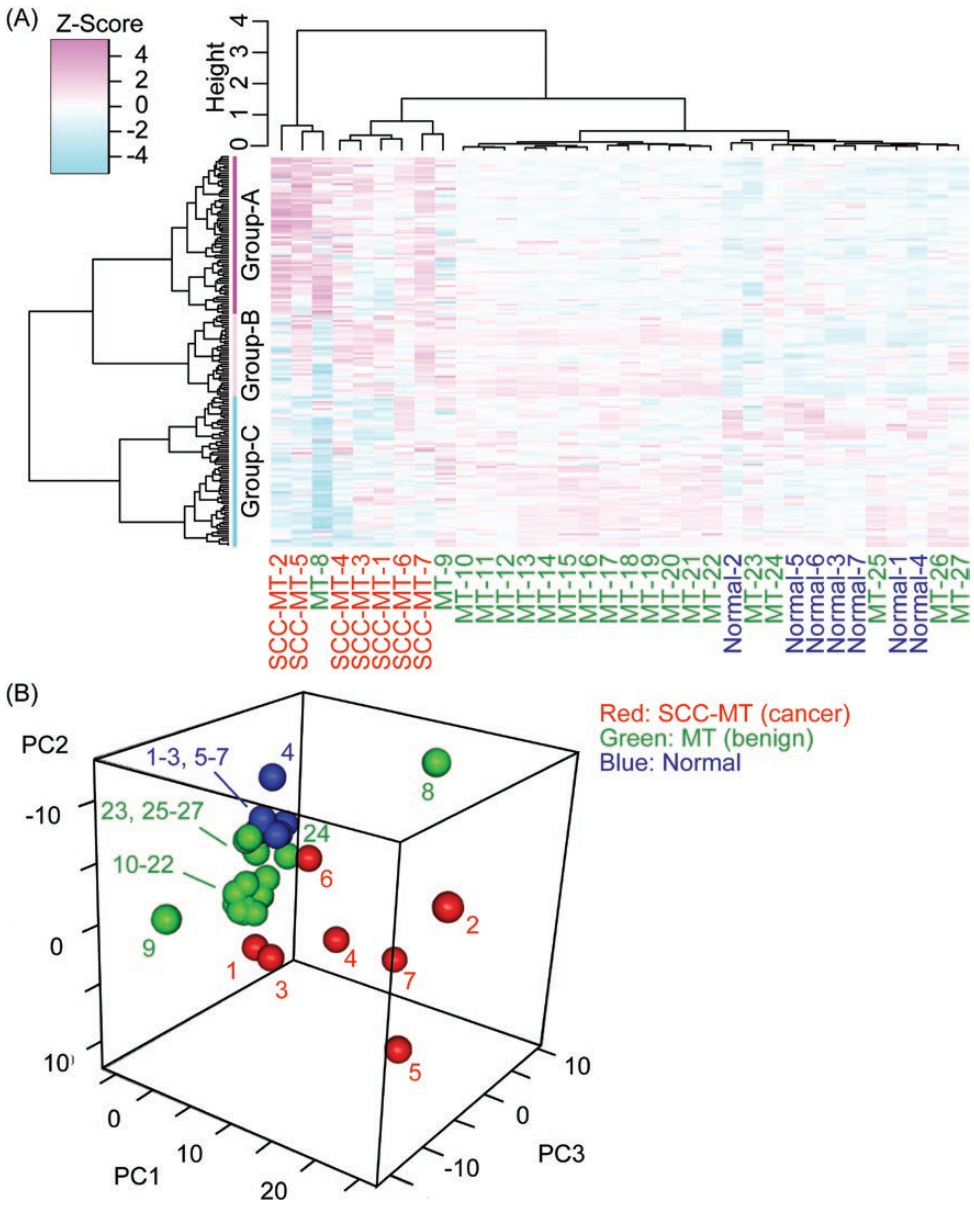

Figure 2. Comprehensive miRNA sequencing using formalin-fixed paraffin-embedded tissues. (**A**) The clustering and heatmap analysis of the miRNA profiling in 7 cancer (SCC-MT-1 to -7) and 7 normal ovary tissues of SCC-MT patients (Normal-1 to -7) and 20 MT tissues of other patients (MT-8 to -27). The normalized data were converted to base 10 logarithms and z-score. (**B**) The principal component analysis of the miRNA profiling in 7 cancer (SCC-MT-1 to -7) and 7 normal ovary tissues of SCC-MT patients (Normal-1 to -7) and 20 MT tissues of other patients (MT-8 to -27).

both miR-151a-3p and miR-378a-3p were also elevated in the murine plasma at 5 weeks post-implantation. Compared with before implantation, miR-151a-3p and miR-378a-3p were elevated 2.10 times and 2.48 times, respectively (Supplementary File 1, available at *Carcinogenesis* Online).

Then we investigated plasma miRNAs of control mice (5 weeks after mock surgery), and these miRNAs were also elevated in the murine plasma of the PDX model at 5 weeks post-implantation compared with the control mice (Supplementary File 2, available at *Carcinogenesis* Online).

Target prediction and functional annotation

Finally, target prediction and functional annotation analysis were performed using the miRSystem to verify the function of the miRNAs. On the basis of the results of FFPE tissues (Figure 3C), we focused on the four SCC-MT–related miRNAs (miR-151a-3p, miR-378a-3p, miR-26a-5p and miR-99a-5p). The functional annotation of the upregulated miRNAs (miR-151a-3p and miR-378a-3p) showed six markedly dysfunctional pathways (Table 2). The target genes in these pathways are shown in Supplementary File 3, available at *Carcinogenesis* Online. Of note, 'protein processing in the endoplasmic reticulum' ($P \leq 0.001$) was the most markedly impaired, and 'nucleotide excision repair' and 'Hedgehog signaling pathway' were also impaired ($P = 0.013$ and $P = 0.021$, respectively). Conversely, 33 were significantly dysfunctional pathways by the downregulated miRNAs (miR-26a-5p and miR-99a-5p). Table 2 and Supplementary File 4, available at *Carcinogenesis* Online present the top ten pathways and the target genes in these pathways, respectively. Compared with the dysfunctional pathway by upregulated miRNAs, several pathways

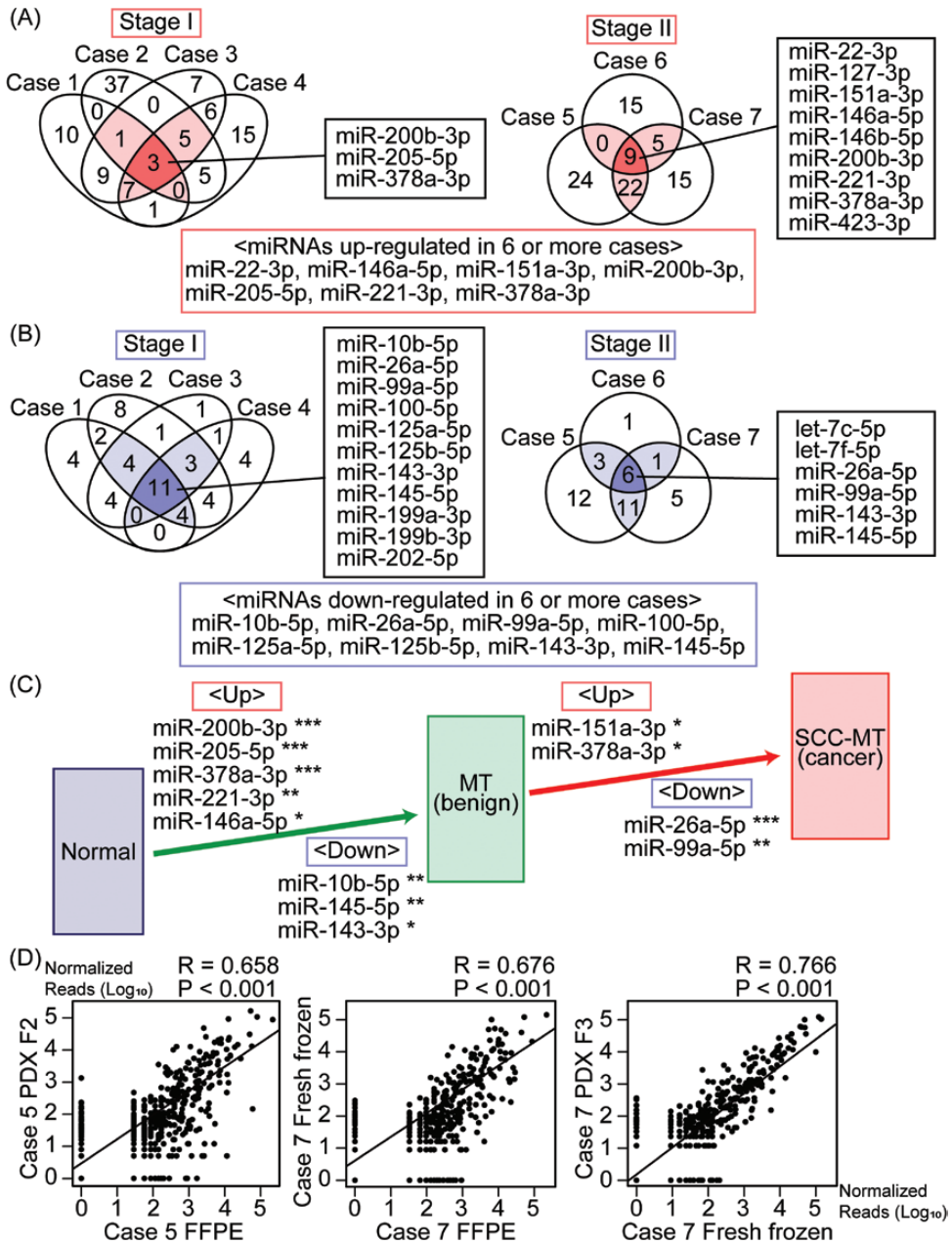

Figure 3. Narrowing down of cancer-related miRNAs and correlations of the miRNA profiling of the FFPE tissues and PDX tissues. (**A**) The number of upregulated miRNAs in cancer of each case (more than delta 1000 reads in normalized reads). The left and right Venn diagrams show upregulated miRNAs in stage I and stage II patients, respectively. (**B**) The number of downregulated miRNAs in cancer of each case (more than delta 1000 reads in normalized reads). The left and right Venn diagrams show downregulated miRNAs in stage I and stage II patients, respectively. (**C**) The comparison of cancer (SCC-MT), normal and MT tissues. Normalized reads of 7 SCC-MT tissues were compared with those of 20 MT tissues, and those of seven 7 tissues were compared with those of 20 MT tissues by a *t*-test (*$P \leq 0.05$, **$P \leq 0.01$, ***$P \leq 0.001$). (**D**) The correlations of FFPE and PDX F_2 tissues of case 5, of FFPE and original fresh-frozen tissues of case 7 and that of fresh-frozen and PDX F_3 tissues of case 7. The normalized data were converted to base 10 logarithms, and the Spearman's correlation coefficient (R) was calculated.

were markedly impaired. In particular, 'pathway in cancer', 'cell cycle', 'mitogen-activated protein kinase signaling pathway' and 'long-term potentiation' were significantly impaired (all *P* values were ≤0.001). Furthermore, 'focal adhesion', 'protein processing in the endoplasmic reticulum' and 'P53 signaling pathway' were significantly impaired ($P = 0.002$, $P = 0.003$ and $P = 0.003$, respectively).

Discussion

As SCC-MT is one of the rare histological subtypes of ovarian carcinoma, limited preliminary research has been conducted, and its pathogenesis remains primarily unclear. In addition, no standard chemotherapy regimen has been established to date, and the prognosis of patients who do not undergo complete surgery remains profoundly poor (2). Hence, further research on SCC-MT is warranted. Reportedly, the p53 overexpression was detected in four cases by immunohistochemistry (11), and alterations in both p53 and p16–Rb pathways have been reported in 21 cases by immunohistochemistry (13). However, another study reported that no mutation of the cyclin-dependent kinase inhibitor 2 (*CDKN2A*) gene, whose impairment could profoundly affect either the $p16^{CDKN2A}$–CyclinD1–pRb cascade or

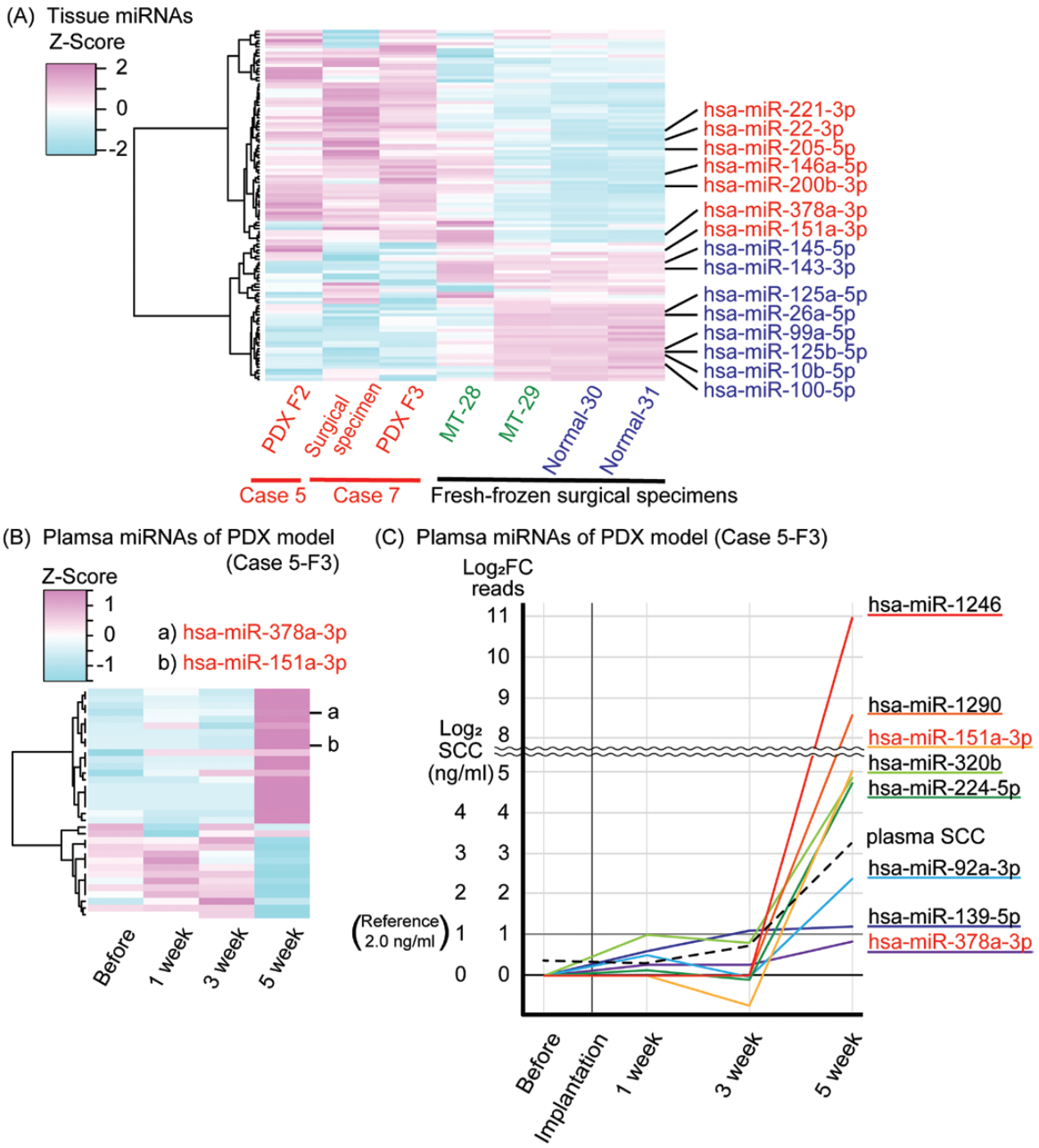

Figure 4. Comprehensive miRNA sequencing using samples of the PDX model. (**A**) The clustering and heatmap analysis of the miRNA profiling in fresh cancer tissues of the PDX model and fresh surgical specimens. Tumor tissues of patients with mature teratoma (MT-28 and -29) and contralateral normal ovary tissues of other patients with benign ovarian tumors (Normal-30 and -31) were used. The normalized data were converted to base 10 logarithms and z-scores. Cancer-related dysregulated miRNAs identified in Figure 2 are shown on the right side. (**B**) The clustering and heatmap analysis of the miRNA profiling in the plasma of the PDX model (case 5-F_3). Murine plasma samples were obtained sequentially (before, 1, 3 and 5 weeks post-implantation), and the normalized data were converted to base 10 logarithms and z-score. (**C**) A line graph of the top eight upregulated miRNAs in the murine plasma of the PDX model (case 5-F_3). Log_2 fold-change of normalized miRNA reads at each point compared with preimplantation is shown. The plasma SCC antigen level is also shown in log base 2 (reference, 2.0 ng/ml).

the $p14^{CDKN2A}$–mdm2–p53 cascade, was observed using fluorescence *in situ* hybridization (14). Recently, like other SCC in the uterine cervix and oropharynx, human papillomavirus was detected by immunohistochemistry and *in situ* hybridization in four cases (15); however, all studies were conducted on a small scale, and, thus, the fundamental biology of this malignancy remains mostly unclear. To the best of our knowledge, this is the first study to investigate the miRNA profiling in SCC-MT using NGS and attempt to elucidate its unknown pathogenesis as well as address the potential applications for diagnostic biomarkers.

Owing to the rarity of SCC-MT, only one fresh-frozen SCC-MT tissues (case 7) was available. Therefore, in this study, FFPE tissues and fresh-frozen tissues of PDX models were used. For initial screening considering individual differences, we used FFPE tissues and compared paired-cancer and normal ovarian tissues of seven patients with SCC-MT. To date, several studies have reported robust correlations between the miRNA expression profiling in matched fresh-frozen and FFPE tissues (27–30); in this study, all normal ovarian tissues exhibited the same expression profiles. Hence, we considered that miRNAs in FFPE tissues were

Table 2. Functional annotation reports of four cancer-related miRNAs using the miRSystem

KEGG Term ID	KEGG Term	*P* value
The upregulated miRNAs (miR-151a-3p and miR-378a-3p)		
4141	Protein processing in endoplasmic reticulum	≤0.001
3420	Nucleotide excision repair	0.013
4340	Hedgehog signaling pathway	0.021
4020	Calcium signaling pathway	0.031
5211	Renal cell carcinoma	0.031
4350	TGF-β signaling pathway	0.042
The downregulated miRNAs (miR-26a-5p and miR-99a-5p)		
5200	Pathways in cancer	≤0.001
4110	Cell cycle	≤0.001
4010	MAPK signaling pathway	≤0.001
4720	Long-term potentiation	≤0.001
5215	Prostate cancer	0.002
4510	Focal adhesion	0.002
4141	Protein processing in endoplasmic reticulum	0.003
4920	Adipocytokine signaling pathway	0.003
4115	P53 signaling pathway	0.003
5211	Renal cell carcinoma	0.004

miRSystem, http://mirsystem.cgm.ntu.edu.tw/; KEGG, Kyoto Encyclopedia of Genes and Genomes; MAPK, mitogen-activated protein kinase; TGF, transforming growth factor.

well preserved. In SCC-MT tissue, we observed various expression profiles, which could be affected by the heterogeneity of SCC-MT. However, the miRNAs annotation rate of case 2 cancer tissue was markedly lower than other samples, and cancer tissues of cases 6 and 7 contained necrotic tissues. Remarkably, two MT tissues (cases 8 and 9) exhibited similar expression profiles to SCC-MT tissues, although the remaining MT tissues exhibited similar trends. However, considering the low incidence of SCC-MT and patients' age, it would be highly unlikely to arise cancer in the two patients with MT in the future even if they did not undergo surgery. Instead, we considered that these MT tissues contained more of a squamous epithelium component because MT comprises well-differentiated tissues derived from the three germ cell layers (ectoderm, mesoderm and endoderm) and has a different ratio of these components in each patient with MT.

On the basis of the results of FFPE tissues, we narrowed down miRNAs and identified four SCC-MT–related miRNAs (Figure 3C). A study reported that, in several breast cancer cell lines, miR-378a-3p was a target of the c-Myc and conferred an oncogenic function by targeting and inhibiting TOB2, a tumor-suppressor candidate and transrepressor of cyclin D1 (31). Reportedly, miR-378 is overexpressed in ovarian cancer cells and tumors (32) and promotes cancer progression in non-small cell lung cancer (33). However, other studies have reported that miR-378a-3p is a tumor suppressor (34,35), and miR-378 is downregulated in oral SCC (36). In some reports, we could not determine whether miR-378 was miR-378a-3p or not (32,33,36). Overall, miR-378a-3p has been reported as both oncogenic and tumor-suppressor miRNA, and the upregulation of miR-378a-3p in SCC-MT was unique. Regarding miR-151a-3p in oncology, only a few studies have been conducted, reporting that miR-151a-3p was one of the p53 target miRNAs (37), and one of the target genes of miR-151a-3p was TWIST1 in breast cancer cells (38). Hence, miR-151a-3p were considered to restore the epithelial phenotype of SCC-MT. Conversely, miR-26a-5p and miR-99a-5p were quite substantially downregulated in SCC-MT compared with MT tissues in this study and were considered to be associated with carcinogenesis. Some studies have reported that both miR-26a-5p and miR-99a-5p are tumor-suppressor miRNAs in several cancer types, including several SCCs (39–43). Thus, like other malignancies, the two downregulated miRNAs were considered to involve the malignant transformation of MT. However, in general, the effect and target genes of miRNAs can be completely different. Therefore, further investigation about the roles of these miRNAs in SCC-MT is desired.

We analyzed fresh tissues of two SCC-MT PDX models and one frozen surgical specimen of case 7 to validate the results of FFPE tissues. As reported earlier, because SCC-MT is a rare type of ovarian tumor, it was difficult to obtain fresh-frozen tissues and serum samples from patients with SCC-MT. The PDX model has been extensively used in cancer research about preclinical drug screening, including novel targeted therapies, biomarker identification and the development of individualized treatment plans, primarily because the histology and oncogene expression are well preserved in PDX models (44,45). In addition, the PDX model could be useful for rare tumor research (46). In this study, the miRNA profiling of FFPE and the corresponding PDX model correlated well, and most dysregulated miRNAs in FFPE were dysregulated in the PDX model. Thus, these miRNAs could be dysregulated in patients with SCC-MT and might play specific roles in their pathogenesis.

Of note, several miRNAs have been observed in the murine plasma, and particularly, both hsa-miR-1246 and -1290 have increased dramatically. These miRNAs were considered to be derived from human cancer tissues because according to miRbase, there are no mouse homologs for them. Reportedly, serum hsa-miR-1246 and -1290 were elevated in uterine cervical SCC (47), whereas hsa-miR-1246 was elevated in esophageal SCC (48). Nevertheless, these miRNAs were not included in the potential biomarker of epithelial ovarian cancer (23,24). Hence, SCC-MT, perhaps, differed from epithelial ovarian cancer, reflecting diversity by the histology of ovarian carcinoma. Remarkably, both miRNA sequencing and qPCR indicated that the expression of miR-378a-3p and miR-151a-3p was also elevated in the murine plasma. According to previous reports, these miRNAs were reported as circulating miRNAs in patients with renal cell carcinoma and gastric cancer (49,50). However, there is the issue

of homology between the human and mouse miRNAs, and it is difficult to distinguish highly conserved miRNAs in this model. In miRNA sequencing, sequences which were annotated as mouse miRNAs were excluded to attenuate the influence of normal mouse tissues. On the other hand, we could not distinguish between human miRNAs and murine miRNAs in qPCR. This might result in the difference between miRNA sequencing and qPCR (Supplementary File 5, available at *Carcinogenesis* Online). Overall, these circulating miRNAs could be potential non-invasive biomarkers of SCC-MT, but further studies using human sample are essential.

Finally, we performed the functional annotation analysis using the miRSystem, which integrates seven well-known miRNA target gene prediction programs—DIANA, miRanda, miRBridge, PicTar, PITA, rna22 and TargetScan—to validate whether these miRNAs were involved in the pathogenesis (26). The functional annotation revealed a robust correlation with several cancer-related pathways, which corroborated studies of each miRNA described earlier. In particular, the identification of 'cell cycle' and 'P53 signaling pathway' was interesting because prior studies about SCC-MT focused on the p53–p21–p16 signaling axis (13,14). Thus, the pathways assumedly played a vital role in SCC-MT. Moreover, several important signaling pathways in cancer biology (mitogen-activated protein kinase, Hedgehog and transforming growth factor-β) have been identified, and, thus, 'pathways in cancer' were impaired in SCC-MT. Hence, the results of the functional annotation were reasonable. As described previously, because miRNA-based effects are tissue specific, the validation in SCC-MT is essential in the future. Overall, the four dysregulated miRNAs, especially miR-26a-5p and miR-99a-5p, supposedly play a specific role in the SCC-MT pathogenesis.

This study has several limitations. First, this study enrolled only seven cases of SCC-MT, although it was a relatively large scale considering the very low incidence of the disease. Thus, comprehensive studies are warranted, along with obtaining samples from multiple institutions. Second, we used FFPE tissues and samples of the PDX model. Reportedly, the miRNA profiling of these cancer tissues might be preserved (27–30,44); however, the validation in fresh surgical tissues from SCC-MT is also exciting. Third, the results of the plasma miRNA could be affected by miRNA derived from mice. Moreover, discussing downregulated miRNAs in the murine plasma was challenging because of the PDX model, and both miR-26a-5p and miR-99a-5p were not annotated in the murine plasma. Thus, circulating miRNAs should be validated in the human serum or plasma, and their clinical benefit as a diagnostic marker should be assessed in the future. Finally, the target genes of cancer-related miRNAs were not validated in this study. Hence, precise target genes should be validated in further analysis to determine their functions.

In conclusion, this study presents the unique miRNA profiling of SCC-MT using NGS for the first time. Moreover, this study suggests the four SCC-MT–related miRNAs and estimated key pathways dysregulated in SCC-MT. We believe that our findings could lead to elucidation of pathogenesis, and could eventually contribute to new treatment strategies. Furthermore, several circulating miRNAs could be potential diagnostic biomarkers; hence, further investigation is desired. We hope to develop an understanding of this rare cancer in the future.

Supplementary material

Supplementary data are available at *Carcinogenesis* online.

Funding

This study was supported by a Japan Society for the Promotion of Science Grant-in-Aid for Scientific Research (17H04338, 16K15704 and 16H02616).

Acknowledgements

We express our highest appreciation to all members of the Department of Drug Safety Sciences, Division of Clinical Pharmacology, and Department of Obstetrics and Gynecology, Nagoya University Graduate School of Medicine. Moreover, we received technical support from the Division for Medical Research Engineering, Nagoya University Graduate School of Medicine. Furthermore, we thank Enago (https://www.enago.jp/) for English editing of this manuscript.

Conflict of Interest Statement: None declared.

References

1. Roth, L.M. *et al.* (2006) Recent advances in the pathology and classification of ovarian germ cell tumors. *Int. J. Gynecol. Pathol.*, 25, 305–320.
2. Hackethal, A. *et al.* (2008) Squamous-cell carcinoma in mature cystic teratoma of the ovary: systematic review and analysis of published data. *Lancet. Oncol.*, 9, 1173–1180.
3. Rathore, R. *et al.* (2018) Malignant transformation in mature cystic teratoma of the ovary: a retrospective study of eight cases and review of literature. *Prz. Menopauzalny*, 17, 63–68.
4. Trabzonlu, L. *et al.* (2017) Malignant tumors associated with ovarian mature teratoma: a single institution experience. *Pathol. Res. Pract.*, 213, 518–521.
5. Kurman, R.J. *et al.* (2014) *WHO Classification of Tumours of Female Reproductive Organs*. 4th edn. IARC press, Lyon.
6. Kikkawa, F. *et al.* (1998) Diagnosis of squamous cell carcinoma arising from mature cystic teratoma of the ovary. *Cancer*, 82, 2249–2255.
7. Chen, R.J. *et al.* (2008) Prognosis and treatment of squamous cell carcinoma from a mature cystic teratoma of the ovary. *J. Formos. Med. Assoc.*, 107, 857–868.
8. Sakuma, M. *et al.* (2010) Malignant transformation arising from mature cystic teratoma of the ovary: a retrospective study of 20 cases. *Int. J. Gynecol. Cancer*, 20, 766–771.
9. Do, V.T. *et al.* (2001) Postoperative concurrent chronomodulated 5-fluorouracil/leucovorin infusion and pelvic radiotherapy for squamous cell carcinoma of the ovary arising from mature cystic teratoma. *Int. J. Gynecol. Cancer*, 11, 418–421.
10. Yoshida, K. *et al.* (2016) Radiotherapy for persistent malignant transformation from mature cystic teratoma of the ovary. *J. Obstet. Gynaecol. Res.*, 42, 584–588.
11. Yoshioka, T. *et al.* (1998) Immunohistochemical and molecular studies on malignant transformation in mature cystic teratoma of the ovary. *J. Obstet. Gynaecol. Res.*, 24, 83–90.
12. Iwasa, A. *et al.* (2007) Squamous cell carcinoma arising in mature cystic teratoma of the ovary: an immunohistochemical analysis of its tumorigenesis. *Histopathology*, 51, 98–104.
13. Iwasa, A. *et al.* (2008) Malignant transformation of mature cystic teratoma to squamous cell carcinoma involves altered expression of p53- and p16/Rb-dependent cell cycle regulator proteins. *Pathol. Int.*, 58, 757–764.
14. Paliogiannis, P. *et al.* (2014) Squamous cell carcinoma arising in mature cystic teratoma of the ovary: report of two cases with molecular analysis. *Eur. J. Gynaecol. Oncol.*, 35, 72–76.
15. Chiang, A.J. *et al.* (2015) Detection of human papillomavirus in squamous cell carcinoma arising from dermoid cysts. *Taiwan. J. Obstet. Gynecol.*, 54, 559–566.
16. Ambros, V. (2004) The functions of animal microRNAs. *Nature*, 431, 350–355.
17. Bartel, D.P. (2004) MicroRNAs: genomics, biogenesis, mechanism, and function. *Cell*, 116, 281–297.

18. Nana-Sinkam, S.P. *et al.* (2011) MicroRNAs as therapeutic targets in cancer. *Transl. Res.,* 157, 216–225.
19. Chen, C.Z. (2005) MicroRNAs as oncogenes and tumor suppressors. *N. Engl. J. Med.*, 353, 1768–1771.
20. Lu, J. *et al.* (2005) MicroRNA expression profiles classify human cancers. *Nature*, 435, 834–838.
21. Tsuchiya, Y. *et al.* (2006) MicroRNA regulates the expression of human cytochrome P450 1B1. *Cancer Res.,* 66, 9090–9098.
22. Motameny, S. *et al.* (2010) Next generation sequencing of miRNAs—Strategies, resources and methods. *Genes (Basel).*, 1, 70–84.
23. Yokoi, A. *et al.* (2017) A combination of circulating miRNAs for the early detection of ovarian cancer. *Oncotarget*, 8, 89811–89823.
24. Yokoi, A. *et al.* (2018) Integrated extracellular microRNA profiling for ovarian cancer screening. *Nat. Commun.*, 9, 4319.
25. Griffiths-Jones, S. *et al.* (2008) miRBase: tools for microRNA genomics. *Nucleic Acids Res.*, 36(), D154–D158.
26. Lu, T.P. *et al.* (2012) miRSystem: an integrated system for characterizing enriched functions and pathways of microRNA targets. *PLoS One*, 7, e42390.
27. Hasemeier, B. *et al.* (2008) Reliable microRNA profiling in routinely processed formalin-fixed paraffin-embedded breast cancer specimens using fluorescence labelled bead technology. *BMC Biotechnol.*, 8, 90.
28. Xi, Y. *et al.* (2007) Systematic analysis of microRNA expression of RNA extracted from fresh frozen and formalin-fixed paraffin-embedded samples. *RNA*, 13, 1668–1674.
29. Zhang, X. *et al.* (2008) An array-based analysis of microRNA expression comparing matched frozen and formalin-fixed paraffin-embedded human tissue samples. *J. Mol. Diagn.,* 10, 513–519.
30. Nam, E.J. *et al.* (2016) Primary and recurrent ovarian high-grade serous carcinomas display similar microRNA expression patterns relative to those of normal ovarian tissue. *Oncotarget*, 7, 70524–70534.
31. Feng, M. *et al.* (2011) Myc/miR-378/TOB2/cyclin D1 functional module regulates oncogenic transformation. *Oncogene*, 30, 2242–2251.
32. Chan, J.K. *et al.* (2014) MiR-378 as a biomarker for response to anti-angiogenic treatment in ovarian cancer. *Gynecol. Oncol.*, 133, 568–574.
33. Chen, L.T. *et al.* (2012) MicroRNA-378 is associated with non-small cell lung cancer brain metastasis by promoting cell migration, invasion and tumor angiogenesis. *Med. Oncol.,* 29, 1673–1680.
34. Xu, Z.H. *et al.* (2018) miR-378a-3p sensitizes ovarian cancer cells to cisplatin through targeting MAPK1/GRB2. *Biomed. Pharmacother.*, 107, 1410–1417.
35. Li, H. *et al.* (2014) Clinical and biological significance of miR-378a-3p and miR-378a-5p in colorectal cancer. *Eur. J. Cancer*, 50, 1207–1221.
36. Scapoli, L. *et al.* (2010) MicroRNA expression profiling of oral carcinoma identifies new markers of tumor progression. *Int. J. Immunopathol. Pharmacol.*, 23, 1229–1234.
37. Bisio, A. *et al.* (2013) Identification of new p53 target microRNAs by bioinformatics and functional analysis. *BMC Cancer*, 13, 552.
38. Yeh, T.C. *et al.* (2016) mir-151-3p targets TWIST1 to repress migration of human breast cancer cells. *PLoS One*, 11, e0168171.
39. Fukumoto, I. *et al.* (2015) MicroRNA expression signature of oral squamous cell carcinoma: functional role of microRNA-26a/b in the modulation of novel cancer pathways. *Br. J. Cancer,* 112, 891–900.
40. Lin, Y. *et al.* (2013) miR-26a inhibits proliferation and motility in bladder cancer by targeting HMGA1. *FEBS Lett.*, 587, 2467–2473.
41. Chang, L. *et al.* (2017) miR-26a-5p suppresses tumor metastasis by regulating EMT and is associated with prognosis in HCC. *Clin. Transl. Oncol.,* 19, 695–703.
42. Sun, J. *et al.* (2013) MicroRNA-99a/100 promotes apoptosis by targeting mTOR in human esophageal squamous cell carcinoma. *Med. Oncol.,* 30, 411.
43. Chen, Y.T. *et al.* (2018) Biological role and clinical value of miR-99a-5p in head and neck squamous cell carcinoma (HNSCC): a bioinformatics-based study. *FEBS Open Bio*, 8, 1280–1298.
44. Dobbin, Z.C. *et al.* (2014) Using heterogeneity of the patient-derived xenograft model to identify the chemoresistant population in ovarian cancer. *Oncotarget*, 5, 8750–8764.
45. Boone, J.D. *et al.* (2015) Ovarian and cervical cancer patient derived xenografts: the past, present, and future. *Gynecol. Oncol.*, 138, 486–491.
46. Sharifnia, T. *et al.* (2017) Emerging opportunities for target discovery in rare cancers. *Cell Chem. Biol.*, 24, 1075–1091.
47. Nagamitsu, Y. *et al.* (2016) Profiling analysis of circulating microRNA expression in cervical cancer. *Mol. Clin. Oncol.,* 5, 189–194.
48. Takeshita, N. *et al.* (2013) Serum microRNA expression profile: miR-1246 as a novel diagnostic and prognostic biomarker for oesophageal squamous cell carcinoma. *Br. J. Cancer,* 108, 644–652.
49. Redova, M. *et al.* (2012) Circulating miR-378 and miR-451 in serum are potential biomarkers for renal cell carcinoma. *J. Transl. Med.*, 10, 55.
50. Liu, H. *et al.* (2012) Genome-wide microRNA profiles identify miR-378 as a serum biomarker for early detection of gastric cancer. *Cancer Lett.*, 316, 196–203.